

Magnetotransport properties of *p*-type carbon-doped ZnO thin films

T. S. Heng,¹ S. P. Lau,^{2,a)} L. Wang,³ B. C. Zhao,³ S. F. Yu,¹ M. Tanemura,⁴ A. Akaike,⁴ and K. S. Teng⁵

¹*School of Electrical and Electronic Engineering, Nanyang Technological University, Singapore 639798, Singapore*

²*Department of Applied Physics, The Hong Kong Polytechnic University, Hung Hom, Kowloon, Hong Kong*

³*Division of Physics and Applied Physics, School of Physical and Mathematical Science, Nanyang Technological University, Singapore 637371, Singapore*

⁴*Graduate School of Engineering, Nagoya Institute of Technology, Gokiso-cho, Showa-ku, Nagoya 466-8555, Japan*

⁵*Multidisciplinary Nanotechnology Centre, School of Engineering, Swansea University, Singleton Park, Swansea SA2 8PP, United Kingdom*

(Received 12 May 2009; accepted 20 June 2009; published online 8 July 2009)

Carbon-doped ZnO (ZnO:C) thin films exhibiting Curie temperature above room temperature were fabricated using ion beam technique. The magnetic moment of the ZnO:C films was found to be around $1.35 \mu_B$ per carbon atom. The ZnO:C films showed *p*-type conduction with a hole concentration of $\sim 5 \times 10^{17} \text{ cm}^{-3}$. In addition, the anomalous Hall effect and negative magnetoresistance can be detected in the ZnO:C films. The magnetotransport properties of the ZnO:C suggested that the films possessed charge carrier spin polarization. © 2009 American Institute of Physics. [DOI: 10.1063/1.3176434]

In recent years, there has been an intense search for ZnO-based ferromagnetic semiconductors with coexistence of ferromagnetic and spin-transport properties, which are desirable for practical spintronics applications.¹ It was predicted that Mn-doped ZnO could exhibit above room temperature (RT) ferromagnetism in a hole-rich environment.² This prediction initiated intensive experimental work on 3*d*-transition metals (TM) doped ZnO. However, the reported results have been receiving skepticism and the origin of the observed ferromagnetism continues to be strongly debated in the literature.³ As a result, this stimulated an extensive experimental and computational search for non-TM doped ZnO, such as carbon-doped ZnO (ZnO:C) as alternatives to fabricate an unambiguous and clean ferromagnetic semiconductor. Pan *et al.*⁴ predicted that hole mediation in ZnO:C film could lead to ferromagnetism, but ZnO:C showed *n*-type behavior experimentally. Thus, the intrinsic ferromagnetism in this carbon system need to be examined carefully before its potential can be explored.

The origin of ferromagnetism in ZnO-based semiconductors is the most unsettled question in today's material community. This complication can be partially alleviated if the magnetotransport properties of these materials can be observed. Anomalous Hall effect (AHE) and magnetoresistance (MR) are among the most important tools to determine practical functionality of the materials as the spin polarized carrier can be probed and controlled electrically,⁵ leading to direct application in electronics. Here, we demonstrate *p*-type ZnO:C films by investigating its ferromagnetic and magnetotransport properties. By tuning the carbon concentration in the ZnO thin films, one can control the strength of ferromagnetic coupling and its magnetotransport properties.

ZnO films with a thickness of 300 nm were prepared on Si substrates at RT using the filtered cathodic vacuum arc technique. The details of ZnO film preparation have been described elsewhere.⁶ The ZnO samples were mounted on a

water-cooled sample holder and subsequently irradiated by Ar⁺ ions at 45° from the normal to the surface using a Kaufman-type ion gun (Iontech Inc. Ltd., model 3–1500–100 FC) with a simultaneous supply of C atoms. For the supply of carbon, a graphite plate located perpendicularly near the ZnO sample was cosputtered with the ZnO sample by Ar⁺ ions with an energy of 500 eV at RT. After the fabrication of ZnO:C films, the samples were cleaned by ethanol prior to characterization.

The structural properties of the as-prepared films were characterized by x-ray diffraction (XRD), x-ray photoemission spectroscopic (XPS), and dispersive x-ray spectroscopy (EDS). The C content of the 4 and 8 min irradiated films were estimated to be ~ 2 and ~ 8 at. %, respectively, as measured by the EDS. The magnetotransport measurements were performed on a Quantum Design physical properties measurement system (PPMS). The van der Pauw method was used to measure the resistivity. The standard four probe method was employed for Hall measurement. The magnetic measurements were carried out with a vibrating sample magnetometer attached to the PPMS system.

The ZnO:C films exhibit a prominent *c*-axis (002) texture at $\sim 34.5^\circ$, corresponding to a ZnO wurtzite structure. No trace of secondary phases, impurities, or graphite-related peaks can be detected within XRD scanning range of 20° to 70°. A shift of (002) peak to higher angles by 0.15° as compared to as-grown ZnO is observed in the ZnO:C. This indicates a reduction in lattice constant *c* with C doping, which is expected as smaller C ions is incorporated into the O sites of ZnO matrices.⁷ XPS measurements confirmed that C has been incorporated into the film.

The magnetic properties of the ZnO:C films were studied at different carbon concentrations. Figure 1(a) shows the magnetic hysteresis loops of the ZnO:C films at 5 and 300 K with 2 and 8 at. % of carbon. All the samples exhibited ferromagnetic ordering above RT with a clear hysteresis loop as shown in the inset of Fig. 1(a). The saturated magnetization (M_s) of the samples varies from 4.21 to 7.84 emu/cm³ at

^{a)}Electronic mail: apsplau@polyu.edu.hk.

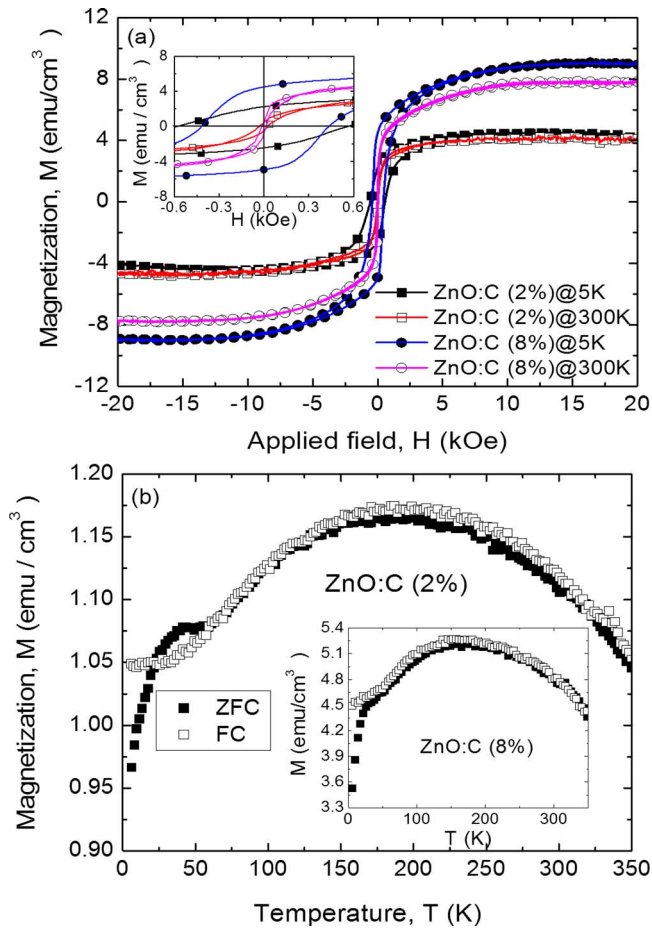


FIG. 1. (Color online) Magnetic properties of ZnO:C films at different carbon concentrations and temperatures. (a) The hysteresis loops of ZnO:C (~ 2 at. %) and ZnO:C (~ 8 at. %) films at 5 and 300 K. The inset of (a) shows the expanded view of the hysteresis loops. (b) The temperature dependence magnetization curves (ZFC and FC) of ZnO:C (2%) and ZnO:C (8 at. %) films.

300 K with C concentration increases from 2 to 8 at. %. At 5 K, the M_s of the ZnO:C samples increased by $\sim 6\%$ to $\sim 15\%$ depending on its C concentration. It is worthwhile to highlight that no ferromagnetism can be observed from the as-grown ZnO and the ion beam irradiated sample in the absence of C plate under identical growth conditions. Considering the estimated C content in the ZnO:C samples, the average M_s at RT is found to be 1.35 and 0.79 μ_B per carbon atom for 2 and 8 at. %, respectively.

The zero-field-cooled (ZFC) and field-cooled (FC) curves for ZnO:C (2 at. % and 8 at. %) films measured under applied field of 1 kOe are shown in Fig. 1(b). All the samples exhibit a Curie temperature above 350 K. The magnetization increases with an increase in temperature up to a transition temperature (T_T) of 216 and 160 K for ZnO:C with 2 and 8 at. % of C, respectively, then the magnetization decreases with temperature greater than T_T . This convex shape of ZFC-FC curve reflects antiferromagnetic and ferromagnetic transition near T_T . For $T_T > 216$ K, a pronounced antiferromagnetic interaction is observed. However, the ferromagnetic phase is still strongly dominant over the whole range of temperatures. It is noted that the ZFC-FC curves are converted into one curve at temperature above ~ 35 K, indicating the absence of superparamagnetism. This rule out the possibility of carbon clusters being the origin of the observed ferromagnetism in the samples. The cusp in the ZFC

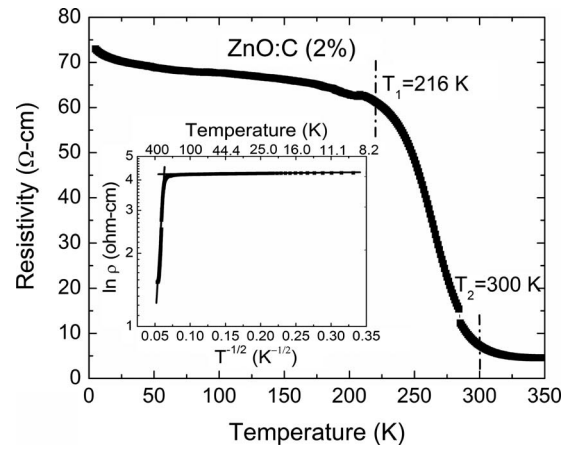


FIG. 2. Temperature dependence of the resistivity on ZnO:C (2 at. %) film. The variable range hopping in the presence of carrier-carrier interaction is evident from the linearity of $\ln(\rho)$ vs $T^{-1/2}$ as shown in the inset, where solid curves are a guide for the eye. The linear fit depicts a transport mechanism and activation energy change at 216 K for the sample.

and FC magnetization is typically interpreted as an indication of spin-glass behavior,⁴ attributing to the frustration originating from the coexistence of ferromagnetic and anti-ferromagnetic interactions.

Unless otherwise stated, the transport measurement was performed on ZnO:C (2 at. %) film because of the relatively low resistivity of the sample. The temperature dependence resistivity $\rho(T)$ of the ZnO:C film is plotted in Fig. 2. The resistivity of the ZnO:C film decreases with increasing temperature. Three distinct $\rho(T)$ regions with its crossover temperatures at 216 K (T_1) and 300 K (T_2) are clearly depicting three different transport mechanisms. For $T > 300$ K, the ZnO:C film exhibits the metalliclike behavior with its resistivity and activation energy keep almost constant at $\sim 3.7 \Omega \text{ cm}$ and $\sim 1.23 \text{ meV}$, respectively. The metallic behavior persisted until T_2 and then followed by a sharp rise in the resistivity up to a temperature of about T_1 , which is reminiscent of a metalliclike to semiconductorlike transition. The ZnO:C possesses resistivity of 62 $\Omega \text{ cm}$ at 216 K. For $T < T_1$, the resistivity increases monotonically. At 30 K, the resistivity of the ZnO:C increases to 70 $\Omega \text{ cm}$ and having an activation energy of 417 meV, elucidating an insulatorlike behavior. Interestingly, we note that the transition temperature of T_1 corresponds well to the ZFC-FC peak of ZnO:C (2 at. %) as illustrated in Fig. 1(b). It suggests that there should be a close correlation between the transport and magnetic properties of the ZnO:C.

In order to further explore the transport mechanism in the ZnO:C, the data were replotted into $\ln(\rho)$ versus $T^{-1/2}$ as shown in the inset of Fig. 2. It is evident that $\ln(\rho)$ is linear as a function of $T^{-1/2}$ with a crossover point at T_1 . The linearity of $\ln(\rho)$ as a function of $T^{-1/2}$ for the entire temperature range is qualitatively consistent with the thermally activated process, $\rho = \rho_0 \exp[(T_0/T)^{1/2}]$, which is a characteristic of magnetic polaron variable range hopping (VRH) in the presence of carrier-carrier interaction.⁸ The VRH mechanism provides a reasonable explanation of transport behavior in ZnO:C films.

Figure 3(a) shows the magnetic-field (H) dependence Hall resistivity (ρ_{xy}) for the ZnO:C film. The field was applied perpendicular to the sample's surface at 300 K as depicted in the inset of Fig. 3(a). As it is common for ferro-

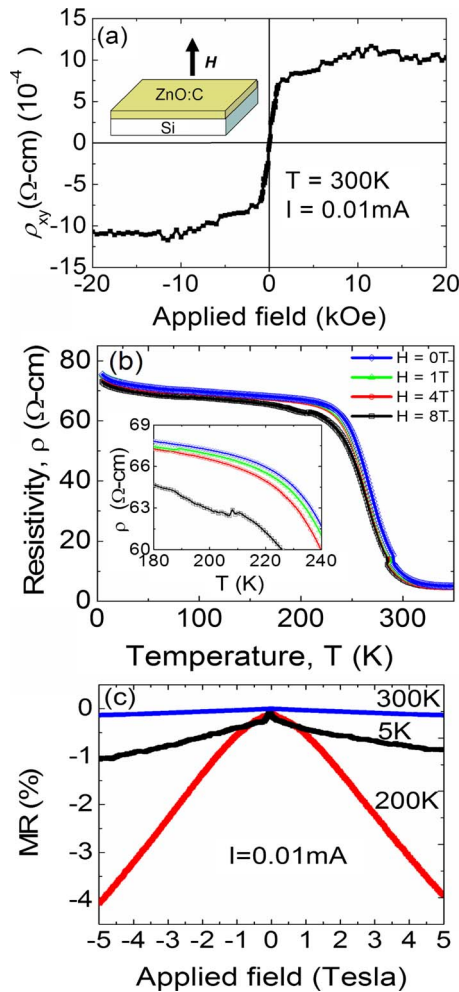


FIG. 3. (Color online) AHE and magnetotransport properties of ZnO:C (2 at. %). (a) The magnetic field dependence of Anomalous Hall resistivity (ρ_{xy}) on the sample measured at 300 K. The applied magnetic field is perpendicular to the sample plane with constant current of 0.01 mA as illustrated in the inset. (b) Temperature dependence resistivity of the sample under an applied field of 0, 1, 4, and 8 Tesla. Inset shows the temperature dependence resistivity from 180 to 240 K. (c) MR curves of the sample measured at 5, 200, and 300 K.

magnetic materials, the value of ρ_{xy} is given by the sum of the ordinary Hall effect and AHE term determined by the magnetization $M(H)$.⁹ At low magnetic fields (<2.5 kOe), ρ_{xy} has largely linear field dependence and the anomalous contribution dominates. Above 2.5 kOe, ρ_{xy} increases gradually and becomes much less field dependent, which is dominated by ordinary Hall resistance. The positive slope at high field regime implies the charge carriers in the ZnO:C is p -type with its hole concentration at $\sim 5.0 \times 10^{17} \text{ cm}^{-3}$. Theoretical calculations suggested that direct hole doping at the anion site such as C substitution on the O site is more effective for localizing the hole and sustaining the magnetic moment.^{4,10} The experimental result is in good agreement with the theoretical prediction. It is worthwhile to highlight that the characteristic of ρ_{xy} as a function of magnetic field is similar to the $M(H)$ plot as shown in Fig. 1(a), suggesting intrinsic nature of ferromagnetism in ZnO:C.

Next, we take into account the magnetotransport properties of the ZnO:C film before discussing the intrinsic nature of this ferromagnetic material. Figure 3(b) shows the temperature dependence of resistivity on the ZnO:C film, per-

formed at applied magnetic fields of 0, 1, 4, and 8 Tesla. The resistivity decreases with an increase in magnetic field, reflecting negative MR. To our surprise, the remarkable change in resistivity occurred in the temperature range between 180 and 240 K, as seen from the inset of Fig. 3(b). It is an unusual phenomenon as compared to TM-doped ZnO materials.³

Figure 3(c) shows the MR curves of the sample at 5, 200, and 300 K, the corresponding MR ratio is -1% , -4% , and -0.2% , respectively. The MR peaked at 200 K and then the value decreases to about 0.2% at 300 K. This unusual result is in accordance with the magnetic dependence $\rho(T)$ data in Fig. 3(b). Combining the magnetic and magnetotransport analysis, the possible underlying mechanism of this unusual MR effect should correlate to the magnetic inhomogeneous and magnetic phase transition at 200 K, as evidenced by $M(T)$ curves in Fig. 1(b). Near transition temperature of 200 K, the ground state changes from ferromagnetic to antiferromagnetic state, leading to domain wall scattering.¹¹ Domain walls are known to be a source of resistance and the phase transition energy goes along with domain walls. Thus, the strongest MR near 200 K could be due to its smaller antiferromagnetic-ferromagnetic transition energy and reduced domain walls resistance. The rapid rise in resistivity from 300 to 200 K could be attributed to the gradual growth of antiferromagnetic interaction, as suggested by the ZFC-FC curve given in Fig. 1(b). Interestingly, the similar MR behavior is found in hole-doped perovskite manganites system such as $\text{La}_{1-x}\text{Sr}_x\text{MnO}_3$, where the highest negative MR ratio occurred at the ferromagnetic transition temperature.¹² Further work is needed to pinpoint the underlying mechanisms for the observed MR behavior in the ZnO:C films.

In summary, we have observed p -type conduction in the ZnO:C film with its hole concentration at $5 \times 10^{17} \text{ cm}^{-3}$. The AHE and MR signals at RT reveal the presence of spin polarization of charge carriers in the films.

This work was partly supported by The Hong Kong Polytechnic University (Project No. 1-ZV95) and the Agency for Science, Technology and Research of Singapore (Project No. 062 101 0030). One of the authors (S.P.L.) is grateful to The Royal Society of the United Kingdom for support through a travel grant.

¹G. A. Prinz, *Science* **282**, 1660 (1998).

²T. Dietl, H. Ohno, F. Matsukura, J. Cibert, and D. Ferrand, *Science* **287**, 1019 (2000).

³C. Liu, F. Yun, and H. Morkoc, *J. Mater. Sci.: Mater. Electron.* **16**, 555 (2005).

⁴H. Pan, J. B. Yi, L. Shen, R. Q. Wu, J. H. Yang, J. Y. Lin, Y. P. Feng, J. Ding, L. H. Van, and J. H. Yin, *Phys. Rev. Lett.* **99**, 127201 (2007).

⁵H. Toyosaki, T. Fukumura, Y. Yamada, K. Nakajima, T. Chikyow, T. Hasegawa, H. Koinuma, and M. Kawasaki, *Nature Mater.* **3**, 221 (2004).

⁶Y. G. Wang, S. P. Lau, H. W. Lee, S. F. Yu, B. K. Tay, X. H. Zhang, K. Y. Tse, and H. H. Hng, *J. Appl. Phys.* **94**, 1597 (2003).

⁷R. D. Shannon, *Acta Crystallogr., Sect. A: Cryst. Phys., Diffr., Theor. Gen. Crystallogr.* **32**, 751 (1976).

⁸M. Foygel, R. D. Morris, and A. G. Petukhov, *Phys. Rev. B* **67**, 134205 (2003).

⁹F. E. Maranzana, *Phys. Rev.* **160**, 421 (1967).

¹⁰X. Peng and R. Ahuja, *Appl. Phys. Lett.* **94**, 102504 (2009).

¹¹P. M. Levy and S. Zhang, *Phys. Rev. Lett.* **79**, 5110 (1997).

¹²A. Urushibara, Y. Moritomo, T. Arima, A. Asamitsu, G. Kido, and Y. Tokura, *Phys. Rev. B* **51**, 14103 (1995).